



Scientific Workshop on Nuclear Fission Dynamics and the Emission of Prompt Neutrons and Gamma Rays, Biarritz, France, 28-30 November 2012

## Isotopic distributions of fission fragments from transfer-induced fission

C. Rodríguez-Tajes<sup>a,\*</sup>, M. Caamaño<sup>a,b</sup>, O. Delaune<sup>a</sup>, F. Farget<sup>a</sup>, L. Audouin<sup>c</sup>, C.-O. Bacri<sup>c</sup>, J. Benlliure<sup>b</sup>, E. Casarejos<sup>b,d</sup>, E. Clement<sup>a</sup>, D. Cortina<sup>b</sup>, X. Derkx<sup>a,e</sup>, A. Dijon<sup>a</sup>, D. Doré<sup>f</sup>, B. Fernández-Domínguez<sup>b</sup>, L. Gaudefroy<sup>g</sup>, C. Golabek<sup>a</sup>, A. Heinz<sup>h</sup>, B. Jurado<sup>i</sup>, A. Lemasson<sup>a</sup>, A. Navin<sup>a</sup>, C. Paradela<sup>b</sup>, D. Ramos<sup>b</sup>, T. Roger<sup>a</sup>, M.D. Salsac<sup>f</sup>, C. Schmitt<sup>a</sup>, K.-H. Schmidt<sup>j</sup>, A. Shrivastava<sup>k</sup>, J. Taieb<sup>g</sup>

<sup>a</sup>GANIL, CEA/DSM-CNRS/IN2P3, BP 55027, F-14076 Caen Cedex 5, France

<sup>b</sup>Universidade de Santiago de Compostela, E-15782 Santiago de Compostela, Spain

<sup>c</sup>Institut de Physique Nucléaire, Université Paris-Sud 11, CNRS/IN2P3, F-91406, Orsay, France

<sup>d</sup>Universidade de Vigo, E-36310 Vigo, Spain

<sup>e</sup>LPC Caen, ENSICAEN, Université de Caen Basse-Normandie, CNRS/IN2P3, 14050 Caen, France

<sup>f</sup>CEA, Irfu, Centre de Saclay, F-91191 Gif-sur-Yvette, France

<sup>g</sup>CEA, DAM, DIF, F-91297 Arpajon, France

<sup>h</sup>Fundamental Fysik, Chalmers Tekniska Högskola, SE-41296, Göteborg, Sweden

<sup>i</sup>Centre d'Études Nucléaires de Bordeaux, Grandignan, Université Sciences et Technologies Bordeaux 1, CNRS/IN2P3, F-33175 Grandignan, France

<sup>j</sup>GSI-Helmholtzzentrum für Schwerionenforschung mbH, D-64220 Darmstadt, Germany

<sup>k</sup>Nuclear Physics Division, Bhabha Atomic Research Centre, Mumbai 400085, India

### Abstract

Fissioning systems from U to Cm as well as  $^{250}\text{Cf}$  were produced by  $^{238}\text{U} + ^{12}\text{C}$  transfer and fusion reactions. The detection of the target-like transfer partner made the characterization of the fissioning systems in (Z,A) and excitation energy possible. The isotopic identification of the fission fragments was achieved by using the VAMOS spectrometer combined to with reactions in inverse kinematics. Results regarding the populated transfer channels and excitation of the target-like transfer partner are presented, as well as the  $^{240}\text{Pu}$  fission probability. Isotopic yields of the fission-fragments for  $^{240,241}\text{Pu}$  and  $^{250}\text{Cf}$ , having excitation energies of about 10 and 45 MeV, respectively, are discussed.

© 2013 The Authors. Published by Elsevier B.V. Open access under CC BY-NC-ND license.

Selection and peer-review under responsibility of Joint Research Centre - Institute for Reference Materials and Measurements

**Keywords:** transfer-induced fission, fission-fragment isotopic yields, trans-uranium actinides, surrogate technique, fission probabilities

**PACS:** 25.70.Gh, 25.70.Hi, 25.85.-w, 27.90.+b

\* Corresponding author: Tel.: +33-231-454-647 ; fax: +33-231-454-665.

E-mail address: rodriguez@ganil.fr

## 1. Introduction

An intense work has been performed during the last decades in order to overcome the restrictions of conventional neutron-induced fission experiments. In this context, the surrogate technique (Escher et al., 2012) was developed in order to estimate those neutron-induced fission cross-sections required for practical applications, which can not be measured directly due to difficulties in producing and handling the required targets. The surrogate method proposes to produce the compound nucleus of interest by an alternative reaction that is accessible in the laboratory. It usually invokes the Weisskopf-Ewing limit, where the branching ratios for the decay of the compound nucleus do not depend on  $(J, \pi)$ , or assumes that both the desired and the surrogate reaction lead to a similar  $(J, \pi)$  population in the compound nucleus. Under these assumptions, the neutron-induced fission cross-section can be obtained as the product of the fission probability measured in the surrogate reaction and the compound-nucleus formation cross-section, which is calculated with an optical potential.

From a more fundamental perspective, the use of alternative reactions is crucial in order to extend the body of available experimental data. An example is the Coulomb-induced fission of radioactive beams, which allowed an unprecedented, extensive survey of low-energy fission for neutron-deficient pre-actinides and actinides (Schmidt et al., 2000) and is the basis of the present SOFIA campaign at GSI (Germany) (Boutoux et al., 2013).

Despite all the efforts dedicated to the understanding of the fission process, the role of neutron and proton shells in the asymmetric fission observed at low excitation energies still remains unclear. Earlier experimental data showed a stabilization of the mass number of the heavy fission fragment at  $A \sim 140$ , which was attributed to the influence of spherical and deformed neutron shells at  $N=82$  and  $N \sim 88$ . However, complementary data from the experiment at GSI (Schmidt et al., 2000) revealed an unexpected stabilization the atomic number at  $Z=54$ , where no proton shell effects are expected (Wilkins et al., 1976). The present work brings new experimental information into this picture, providing a simultaneous measurement of both the mass and atomic number of one of the fission fragments (either the heavy or the light one) through a new experimental technique that combines  $^{238}\text{U} + ^{12}\text{C}$  transfer-induced fission reactions and inverse kinematics. Recent data regarding the populated reaction channels and earlier measurements devoted to the study of the fission fragments (Farget et al., 2012) will be discussed.

## 2. Experiment

A  $^{238}\text{U}^{31+}$  beam with an average intensity of  $10^9$  pps was accelerated in the CSS1 cyclotron of GANIL up to 6.14 MeV/u and impinged on a  $100 \mu\text{g}/\text{cm}^2$ -thick  $^{12}\text{C}$  target, the incident energy in the centre of mass being 10 % above the Coulomb barrier. Inelastic, fusion and transfer reactions were observed in the exit channel, producing a wide variety of excited actinides with a certain probability of decaying by fission.

The detection of the target-like nucleus was performed in a silicon telescope named SPIDER, which covered polar angles between  $30^\circ$  and  $47^\circ$ . SPIDER is composed by two double-sided, annular, Si detectors,  $70 \mu\text{m}$  and  $1 \text{ mm}$ -thick. They were used to measure the energy loss,  $\Delta E$ , and the residual energy,  $E_{res}$ , giving the total kinetic energy  $E = \Delta E + E_{res}$ . The  $\Delta E - E$  correlation was used to identify the target-like nucleus in  $(Z, A)$  and, therefore, the complementary actinide, assuming a two-body reaction. The scattering angle of the target-like nucleus was measured with an uncertainty below  $1^\circ$  thanks to the segmentation of the telescope, making possible the determination of the excitation energy with a final resolution of 2.8 MeV (FWHM).

The large-acceptance VAMOS spectrometer was used for the simultaneous measurement of one of the fission fragments, which is described in detail in Ref. (Farget et al., 2012). The energy loss and the residual energy of the fragment, measured in an ionization chamber and a Si wall, were used to reconstruct its total kinetic energy and identify the atomic number by means of the  $\Delta E - E$  correlation, with  $\Delta Z/Z = 1.5 \cdot 10^{-2}$ . Vertical and horizontal position measurements performed in two drift chambers after the VAMOS dipole were used to reconstruct the magnetic rigidity, the path and the angles at the target position by an ion-optical procedure (Pullanhiotan et al., 2008). In addition, time-of-flight measurements were performed with a secondary-electron detector, using the high frequency of the cyclotron as time reference, and the fragment mass was determined via the E-TOF-Bp technique with a resolution  $\Delta A/A = 0.8 \cdot 10^{-2}$ .

Finally, six clovers of the EXOGAM array of Ge detectors surrounded the target for coincident  $\gamma$ -ray measurements,

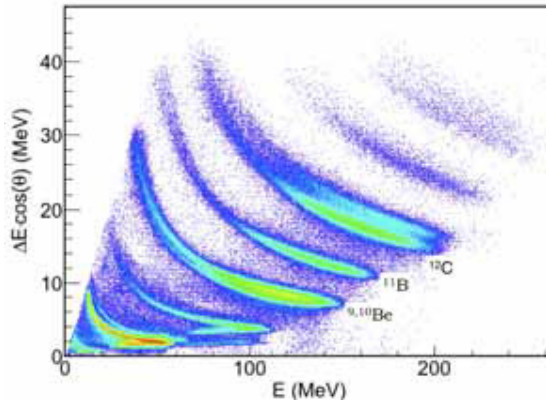


Fig. 1. Identification of the target-like nuclei from the  $\Delta E - E$  measurements provided by SPIDER. A condition requiring a simultaneous detection of a fission fragment in VAMOS was applied to the data.

which were used to cross-check the identification of the fission fragments and investigate the excitation of target-like nuclei in the exit channel.

### 3. Analysis of the target-like nuclei

Figure 1 shows the isotopic identification of the target-like nuclei achieved from the  $\Delta E - E$  correlation provided by SPIDER. Fissioning systems between U and Cm were produced, corresponding to the transfer of up to eight nucleons between the projectile and the target. The angular distributions measured for the different transfer channels show a similar bell shape centred at an approximate angle of  $37^\circ$  in the laboratory, which is above the calculated grazing angle of  $30^\circ$ . In general, integrated transfer cross-sections, corresponding to the SPIDER angular range, decrease exponentially with the opposite of the ground-state Q-value,  $-Q_{gs}$ , and the number of transferred nucleons (Biswas et al., 1995), amounting to few tens of mb for the strongest channels. The excitation-energy distribution measured for  $^{238}\text{U}(^{12}\text{C}, ^{10}\text{Be})^{240}\text{Pu}$  is shown in Fig. 2. The fission probability is also presented and, although corrections from the VAMOS acceptance still need to be applied, main features, such as the onset of first and second chance fission, are visible at approximate excitation energies of 6 and 14 MeV, respectively.

Gamma-ray spectra of the target-like nuclei are given in Fig. 3 for inelastic,  $^{238}\text{U}(^{12}\text{C}, ^{11}\text{B})^{239}\text{Np}$  and  $^{238}\text{U}(^{12}\text{C}, ^{10}\text{Be})^{240}\text{Pu}$  reactions. Among those events with an excitation energy above the first excited state of the target-like nuclei,  $\gamma$ -ray emission from this state was observed with a fraction of  $13 \pm 3\%$  for the three cases. This result indicates that excitation of the target-like nuclei, which is usually neglected in the measurement of fission probabilities and application of the surrogate technique, can be important.

### 4. Analysis of the fission-fragments

Two different systems were analysed:  $^{240,241}\text{Pu}$  with an excitation-energy distribution centred at 10 MeV and  $^{250}\text{Cf}$ , with an excitation energy of 45 MeV. The isotopic fission-fragment yields determined for both cases are given in Fig. 4 (left) as a function of the mass of the fragment and reflect the evolution from asymmetric to symmetric fission with the increase of excitation energy. The good agreement between the results obtained for  $^{240,241}\text{Pu}$  and previous measurements available from thermal-neutron-induced fission of  $^{239}\text{Pu}$  ( $E_x \sim 6$  MeV) (Schmitt et al., 1984), (Bail, 2009) proves the validity of our method (Fig. 4, top-right). The fragment yields measured for  $^{250}\text{Cf}$  were also investigated as a function of the atomic number and are shown in Fig. 4 (bottom-right). The absence of proton emission expected at moderate excitation energies (45 MeV) is reflected in the experimental Y(Z) distribution, which, within an accuracy

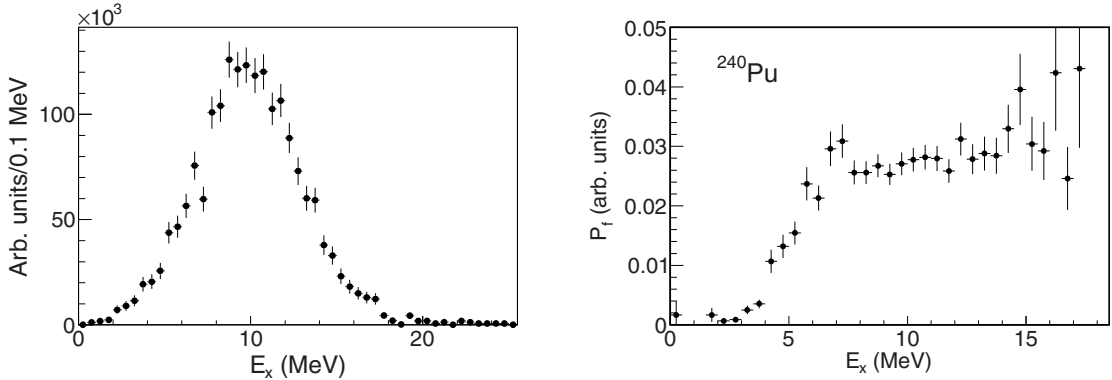


Fig. 2. (Left) Excitation energy distribution measured for  $^{240}\text{Pu}$ . (Right) Fission probability measured for  $^{240}\text{Pu}$ . Experimental results still need to be corrected from the acceptance of the VAMOS spectrometer.

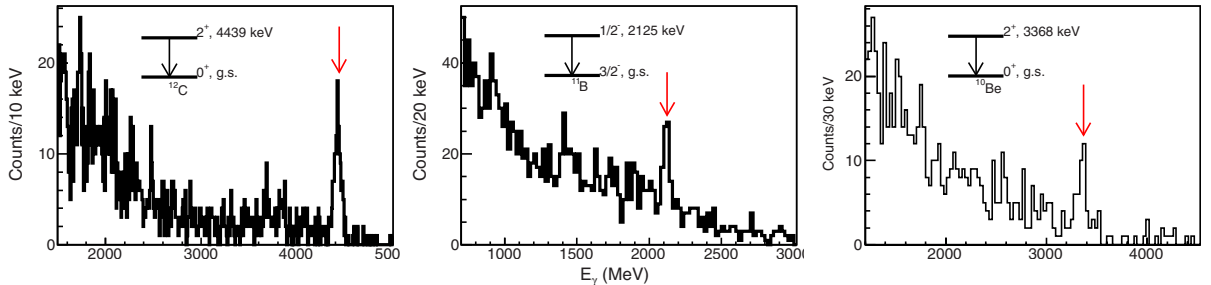


Fig. 3.  $\gamma$ -ray spectra of the target-like nuclei in the exit channel of inelastic (left),  $(^{12}\text{C}, ^{11}\text{B})$  (center) and  $(^{12}\text{C}, ^{10}\text{Be})$  (right) reactions.

of 10 %, shows equal yields for complementary atomic numbers, i.e.  $Z_1+Z_2=98$ . The central plateau observed in the experimental data disagrees with the expected Gaussian shape. It was interpreted as a consequence of the contributions of lighter Cf isotopes produced by pre-scission neutron evaporation, which decreases the excitation energy of the fissioning systems. GEF calculations (Schmidt and Jurado, 2010) where equal contributions of  $^{245-250}\text{Cf}$  were considered nicely reproduce the experimental data.

Figure 5 shows the fission-fragment neutron excess, defined for each atomic number as  $\langle N(Z) \rangle / Z$ , where  $\langle N(Z) \rangle$  is the average neutron number for a given  $Z$ . In the case of  $^{240,241}\text{Pu}$ , the observed saw-tooth behaviour is produced by structure effects of the heavy fragment and post-scission neutron evaporation. The main feature appears at  $Z=50$  and is associated with the formation of the spherical, doubly-magic nucleus  $^{132}\text{Sn}$ , for which neutron emission is suppressed. The fact that the experimental results are well reproduced by GEF simulations shows the accuracy of this code for the description of the microscopic features of the fission process. Measurements carried out for  $^{250}\text{Cf}$  reveal a constant neutron excess, independent of the atomic number of the fragments, which is compatible with a total neutron evaporation (pre- and post-scission) of nine neutrons. However, GEF simulations predict an increase of the neutron excess for heavier fragments, known as charge polarization. The absence of charge polarization found for  $^{250}\text{Cf}$  points out a new feature of the fission process that requires further investigation and may be related to the sharing of excitation energy between the two fission fragments.

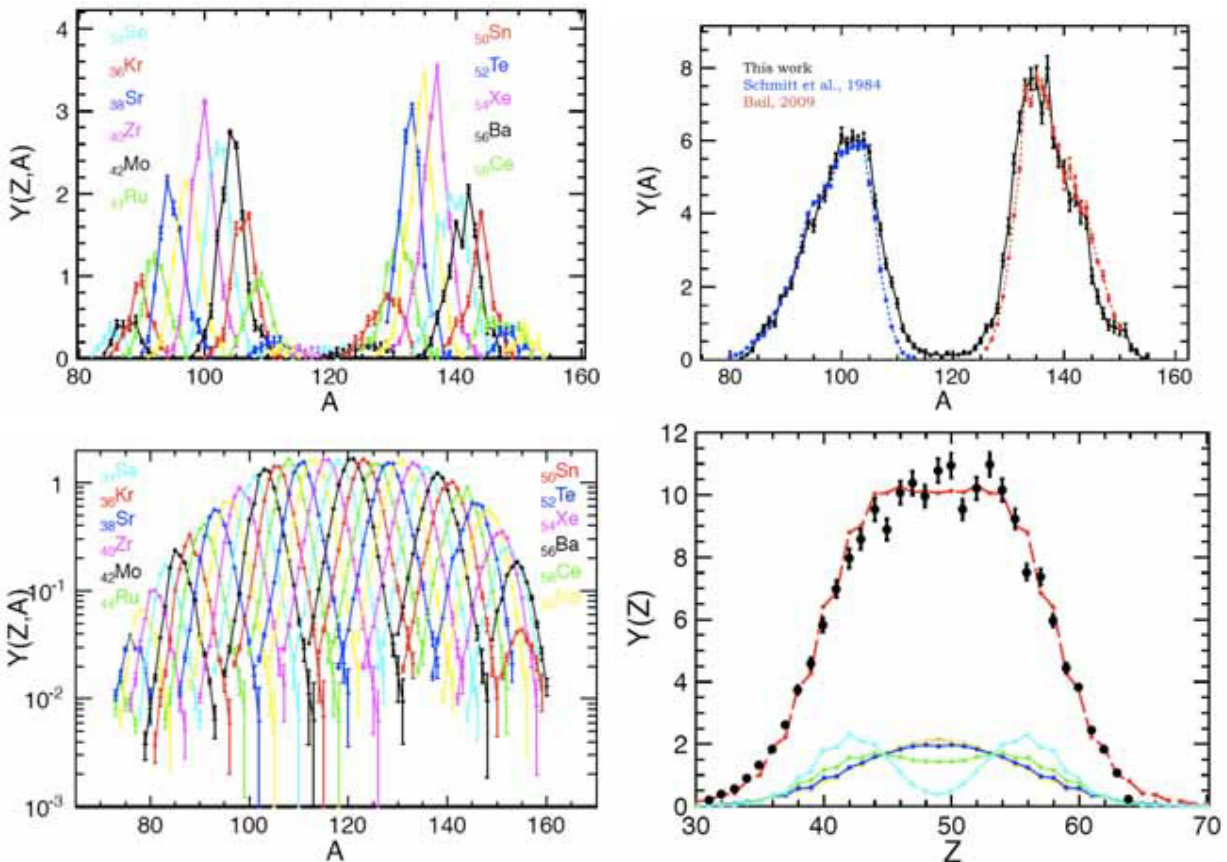


Fig. 4. (Top, left) Experimental isotopic yields of the fission fragments for  $^{240,241}\text{Pu}$  as a function of the fragment mass. (Top, right) Comparison of the  $^{240,241}\text{Pu}$  results obtained in this work, in black, with previous ( $\eta_h, ^{239}\text{Pu}+\text{f}$ ) measurements. (Bottom, left) Experimental isotopic yields of the fission fragments for  $^{250}\text{Cf}$  as a function of the fragment mass. (Bottom, right) Fission-fragment yields as function of the atomic number for  $^{250}\text{Cf}$ . The experimental data were normalized to 200. The solid lines represent calculated yields arriving from the fission of  $^{245-250}\text{Cf}$ . The red line is the sum of  $^{245-250}\text{Cf}$  contributions, assuming equal probabilities.

## 5. Summary and conclusions

An experimental campaign was developed at GANIL where  $^{238}\text{U}+^{12}\text{C}$  transfer-induced fission reactions were studied in inverse kinematics, allowing the investigation of fissioning systems between U and Cf, as well as  $^{250}\text{Cf}$ , produced in fusion reactions. Recent data taken during our last experiment provided a complete characterization of the produced fissioning systems and made a detailed investigation of the angular and excitation energy distributions populated in each transfer channel possible, as well as integrated transfer cross-sections and fission probabilities. For the first time, experimental data are available that provide access to the excitation of the target-like nucleus in the exit channel. A non-negligible probability of populating excited states of the target-like partner was observed, which needs to be considered for the application of the surrogate technique.

Earlier experimental results probed the potential of this new approach to the investigation of the fission process, which allows an accurate and complete measurement of the fission-fragment isotopic yields for both the light and the heavy fragment. The investigation of the neutron excess of the fragments at low excitation energies carried out for  $^{240,241}\text{Pu}$  clearly reflects nuclear-structure effects of the nascent heavy fragment at  $Z=50$ , while results obtained at higher excitation for  $^{250}\text{Cf}$  reveal an unexpected constant behaviour with the atomic number of the fragments, which certainly deserves further investigation.

Finally, new experimental data regarding the fission fragments will be available from our last experiment for an

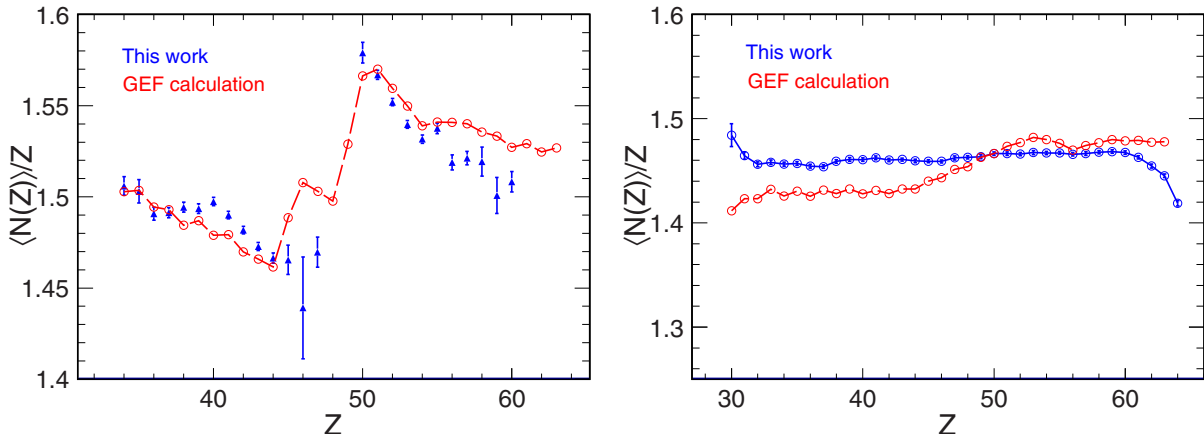


Fig. 5. Neutron excess of the fission fragments as a function of the atomic number for the  $^{240,241}\text{Pu}$  (left) and  $^{250}\text{Cf}$  (right) systems, with excitation energies of 10 and 45 MeV, respectively. The experimental data are represented together with GEF predictions, in red.

extended number of fissioning systems with improved statistics, that will deepen the previous results and investigate the fission yields as a function of the excitation energy.

## Acknowledgments

This work was partially supported by: Spanish Ministry of Education, under a fellowship for postdoctoral mobility (2011) administered by FECYT; Région Basse Normandie with a Chair of Excellence position in GANIL; EURATOM programme under contract 44816; EURATOM/FP7-249671.

## References

- Bail, A., 2009. Mesures de rendements isobariques et isotopiques des produits de fission lourds sur le spectromètre de masse Lohengrin. PhD dissertation. University of Bordeaux 1.
- Boutoux, G., 2013. This conference proceedings.
- Biswas, D.C., Choudhury, R.K., Nadkarni, D.M., Ramamurthy, V.S., 1995. Evidence of massive cluster transfers in  $^{19}\text{F}+^{232}\text{Th}$  reaction at near barrier energies. *Physical Review C* 52, R2827–R2830.
- Escher, J.E., Burke, J.T., Dietrich, F.S., Scielzo, N.D., Thompson, I.J., Younes, W., 2012. Compound-nuclear reaction cross sections from surrogate measurements. *Reviews of modern physics* 84, 353–397.
- Farget, F., Caamaño, M., Delaune, O., Tarasov, O.B., Derkx, X., Schmidt, K.-H., Amthor, A.M., Audouin, L., Bacri, C.-O., Barreau, G., Bastin, B., Bazin, D., Blank, B., Benlliure, J., Caceres, L., Casarejos, E., Chibihi, A., Fernandez-Dominguez, B., Gaudefroy, L., Golabek, C., Grevy, S., Jurado, B., Kamalou, O., Lemasson, A., Lukyanov, S., Mittig, W., Morrissey, D.J., Navin, A., Pereira, J., Perrot, L., Rejmund, M., Roger, T., Saint-Laurent, M.-G., Savajols, H., Schmitt, C., Sherill, B.M., Stodel, C., Taieb, J., Thomas, J.C., Villari, A.C., 2012. Isotopic fission fragment distributions as a deep probe to fusion-fission dynamics. *Journal of Physics: Conference Series* - 11th International Conference on Nucleus-Nucleus Collisions. San Antonio-Texas, EEUU. arXiv:1209.0816.
- Pullanhiotan, S., Rejmund, M., Navin, A., Mittig, A.W., Bhattacharyya, S., 2008. Performance of VAMOS for reactions near the Coulomb barrier. *Nuclear Instruments and Methods A* 593, 343.
- Schmitt, C., Guessous, A., Bocquet, J.P., Clerc, H.-G., Brissot, R., Engelhardt, D., Faust, H.R., Gönnenwein, F., Mutterer, M., Nifenecker, H., Pannicke, J., Ristori, C.H., Theobald, J.P., 1984. Fission yields at different fission-product kinetic energies for thermal-neutron-induced fission of  $^{239}\text{Pu}$ . *Nuclear Physics A* 430, 21–60.
- Schmidt, K.-H., Steinhäuser, S., Böckstiegel, C., Grewe, A., Heinz, A., Junghans, A.R., Benlliure, J., Clerc, H.-G., de Jong, M., Müller, J., Pfützner, M., Voss, B., 2000. Relativistic radioactive beams: A new access to nuclear-fission studies. *Nuclear Physics A* 665, 221–267.
- Schmidt, K.-H., Jurado, B., 2010. General model description of fission observables. Technical report, CENBG, CNRS/IN2P3. <http://www.cenbg.in2p3.fr/GEF>.
- Wilkins, B.D., Steinberg, E.P., Chasman, R.R., 1976. Scission-point model of nuclear fission based on deformed-shell effects. *Physical Review C* 14, 1832–1863.